IJUS

International Journal of Unconventional Science
issue 15–16(5), pp.143–150, 2017

received: 31.07.17
accepted: 09.08.17
http://www.unconv-science.org/n15/kernbach3
DOI: https://doi.org/10.17613/zh5b-jd94

On metrology of electrochemical impedance spectroscopy in time-frequency domain

[1]S.Kernbach, I.Kuksin, O.Kernbach, A.Kernbach

***Abstract*—The paper briefly considers the metrology of electrochemical impedance spectroscopy (EIS) in time-frequency domain for analysis of nonstationary processes in liquids and organic tissues. In particular, the application of normalization operator to satisfy the stationarity condition in impedance calculation is discussed. It introduces new measurement scales as inverse functions of time $func(t)^{-1}$ and frequency-time $func(f,t)^{-1}$ or operates in dimensionless units. Such normalization shifts the focus of EIS from electrochemical test systems to external excitations affecting samples. This provides universality required for characterization of chemical, biological and biophysical interactions of different nature. Reproducible calibration of EIS devices for standardization of such measurements is described. The discussed approach is exemplified by differential EIS measurements in thermostabilized system with excitation of fluidic samples in thermal and optical way.**

I. Introduction

Electrochemical impedance spectroscopy (EIS) is a well-known method of physicochemical analysis in laboratory, field and industrial environments [1], [2]. Typically, EIS is used for analysis of electrotechnical systems, battery and electrolytes, surface and ionic phenomena, and several other effects [3]. The first applications of this method for measuring ionic properties of organic solutions and biological tissues in the framework of biophysics and early spintronics date back to the 80s [4]. At present, the EIS is developed further, in particular, the impedance spectroscopy is applied not only in the frequency domain, but also in the time-frequency domain. Such EIS measurements are carried out with exposition of fluids by external excitations without removing electrodes from measuring containers, see Fig. 1. The sensory element is represented not only by physicochemical properties of fluids, but also by electrochemical interactions during measurements (e.g. change of ionic reactivity). As currently assumed, these interactions utilize quantum mechanisms on the level of ion production and proton conductivity [5], [6], [7]. This methodology significantly increases the sensitivity and resolution of the sensor, as well as minimizes interferences.

Fig. 1. The differential EIS spectrometer, 1,2,3 – elements of the device; 4, 5 – electrodes of the channel 1 and 2.

Measurements in the time-frequency domain extend the EIS paradigm for investigating nonstationary processes in aqueous and colloidal solutions, and in organic tissues. In this case, it is common to consider the electrochemical measurement system as a linear stationary system for small signals with discrete time [8]. The analysis is performed by the frequency response analysis (FRA), as well as by processing the RMS excitation and response signals [9]. Both methods are implemented in the EIS device and in the measurement methodology.

The time-frequency EIS introduces a new scale and it is necessary to consider metrological aspects of these measurements. First of all, the question arises about the meaning of used measurement scales and calibration of EIS devices. The following sections consider the application of dimensionless, inverse functions of time $func(t)^{-1}$ or frequency-time $func(f,t)^{-1}$ scales. We argue that all three options reflect the same principle of relative measurements, where the focus is shifted from electrochemical test systems to external excitations affecting fluidic and organic samples [10]. This approach allows considering a common nature of different chemical, biological and biophysical interactions. Since Prof. Vernadsky was one of the first researchers, who expressed in 1931 [11] the idea of a common unit in measuring various biophysical processes, it is proposed to support the initiative of naming this scale as the Vernadsky scale.

[1]CYBRES GmbH, Research Center of Advanced Robotics and Environmental Science, Melunerstr. 40, 70569 Stuttgart, Germany, Contact author: *serge.kernbach@cybertronica.de.com*. This is translated and revised version of the original paper appeared in IJUS, 15–16(5), 143–150, 2017.

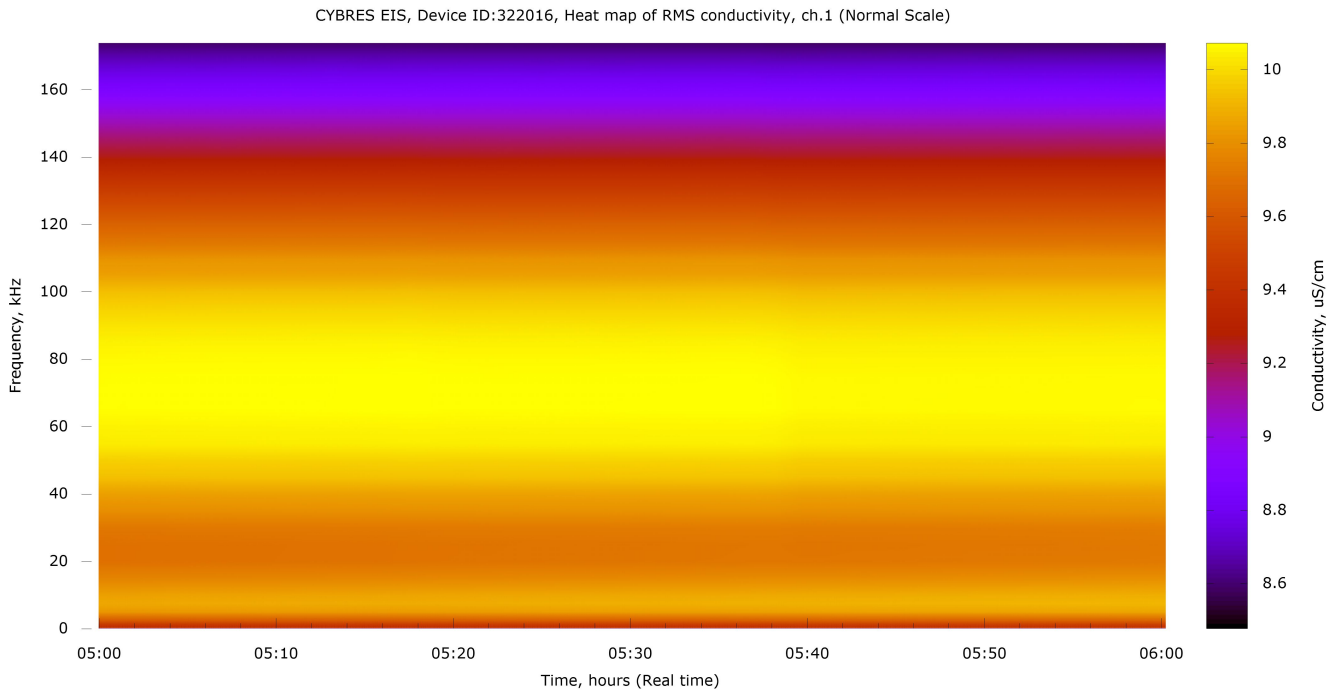

Fig. 2. Graphical representation of the tensor ${}^{k}\Upsilon_{t}^{f}$ (1) as the heat map (RGB color palette), the conductivity of water is measured in the frequency range 0.1kHz–170kHz.

II. Spectroscopy in the time-frequency domain

The result of EIS analysis in the time-frequency domain is represented by the third-rank tensor ${}^{k}\Upsilon_{t}^{f}$ with discrete indices k, f, t. The f, t denote the frequency and time components, the index k denotes the components of EIS analysis (magnitude, phase, correlation, real and imaginary parts of the FRA, etc.), see [12] on the tensor notation. The dimension ${}^{k}\Upsilon_{t}^{f}$ causes difficulties for its representation, one of the possibilities is to use the heat map graphs, where t, f are located on the axes x, y, and the color scale represents one of k, see Fig. 2. The tensor ${}^{k}\Upsilon_{t}^{f}$ has the following form

$$\left.\begin{array}{cccc|cccc} {}^{k}\Upsilon_{t_0}^{f_{max}} & {}^{k}\Upsilon_{t_1}^{f_{max}} & \dots & {}^{k}\Upsilon_{t_{m-1}}^{f_{max}} & {}^{k}\Upsilon_{t_m}^{f_{max}} & {}^{k}\Upsilon_{t_{m+1}}^{f_{max}} & \dots & {}^{k}\Upsilon_{t_{max-1}}^{f_{max}} & {}^{k}\Upsilon_{t_{max}}^{f_{max}} \\ {}^{k}\Upsilon_{t_0}^{f_{max-1}} & {}^{k}\Upsilon_{t_1}^{f_{max-1}} & \dots & {}^{k}\Upsilon_{t_{m-1}}^{f_{max-1}} & {}^{k}\Upsilon_{t_m}^{f_{max-1}} & {}^{k}\Upsilon_{t_{m+1}}^{f_{max-1}} & \dots & {}^{k}\Upsilon_{t_{max-1}}^{f_{max-1}} & {}^{k}\Upsilon_{t_{max}}^{f_{max-1}} \\ \dots & \dots & \dots & \dots & \dots & \dots & \dots & \dots & \\ {}^{k}\Upsilon_{t_0}^{f_2} & {}^{k}\Upsilon_{t_1}^{f_2} & \dots & {}^{k}\Upsilon_{t_{m-1}}^{f_2} & {}^{k}\Upsilon_{t_m}^{f_2} & {}^{k}\Upsilon_{t_{m+1}}^{f_2} & \dots & {}^{k}\Upsilon_{t_{max-1}}^{f_2} & {}^{k}\Upsilon_{t_{max}}^{f_2} \\ {}^{k}\Upsilon_{t_0}^{f_1} & {}^{k}\Upsilon_{t_1}^{f_1} & \dots & {}^{k}\Upsilon_{t_{m-1}}^{f_1} & {}^{k}\Upsilon_{t_m}^{f_1} & {}^{k}\Upsilon_{t_{m+1}}^{f_1} & \dots & {}^{k}\Upsilon_{t_{max-1}}^{f_1} & {}^{k}\Upsilon_{t_{max}}^{f_1} \\ {}^{k}\Upsilon_{t_0}^{f_0} & {}^{k}\Upsilon_{t_1}^{f_0} & \dots & {}^{k}\Upsilon_{t_{m-1}}^{f_0} & {}^{k}\Upsilon_{t_m}^{f_0} & {}^{k}\Upsilon_{t_{m+1}}^{f_0} & \dots & {}^{k}\Upsilon_{t_{max-1}}^{f_0} & {}^{k}\Upsilon_{t_{max}}^{f_0}. \end{array}\right. \quad (1)$$

The tensor ${}^{k}\Upsilon_{t}^{f}$ is structured with respect to the indices t for the areas before and after the time t_m

$$A: \quad {}^{k}\Upsilon_{t}^{f} \rightarrow \quad t < t_m, \quad (2)$$

$$B: \quad {}^{k}\Upsilon_{t}^{f} \rightarrow \quad t \geq t_m, \quad (3)$$

where t_m represents the begin of exposure, A is the background measurement area, and B is the area, where the response is analyzed.

An essential issue of ${}^{k}\Upsilon_{t}^{f}$ in relation to components f is the superposition of the response of EIS system U_{EIS} and the response of a fluidic test object U_{object}

$${}^{k}\Upsilon^{f=f_0 \dots f_{max}} = U_{EIS}^{f} U_{object}^{f}. \quad (4)$$

In some EIS systems [13] a linear character U_{EIS}^{f} of f is assumed and an offset calibration for $f = f_0 \dots f_{max}$ is performed. This leads U_{EIS}^{f} to 1 for all f. However, the real properties of U_{EIS}^{f} are non-linear. Thus, the expression (4) results in a non-linear sensitivity that is manifested in different scales for each of f. This effect is well visible in Fig. 2, where the difference between f is larger than the variation of the signal inside one f.

The behavior of ${}^{k}\Upsilon_{t}^{f}$ in relation to the components t results in nonlinearity, due to the fact that EIS interacts with the test system during measurements

$${}^{k}\Upsilon_{t=t_0 \dots t_{max}} = O_{t}^{EIS}\left(O_{t}^{object}, t\right). \quad (5)$$

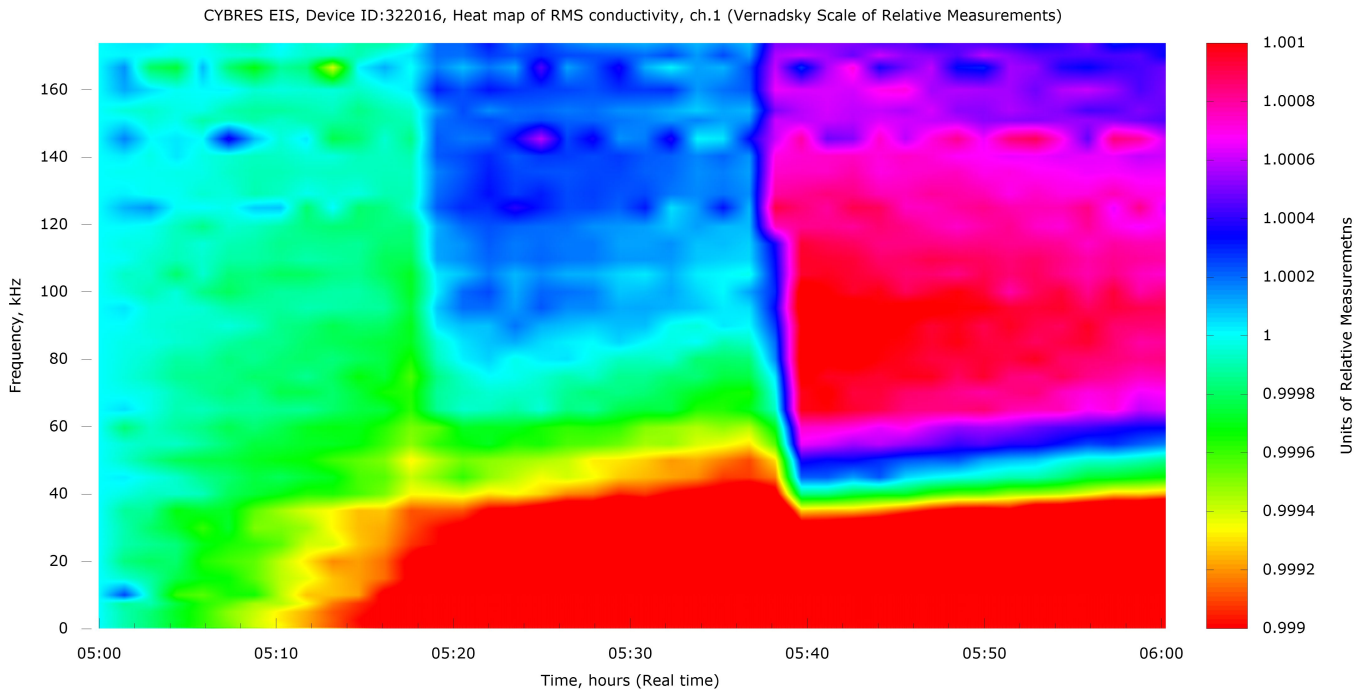

Fig. 3. The normalized representation of the tensor ${}^k\Upsilon_t^f$ by (8). The same graph as in Fig. 2, but represented in the URM (Units of Relative Measurements) scale, the color palette HSV, the resolution $2 \cdot 10^{-3}$ URM for the entire scale, conductivity fluctuations at 10^{-4} are well visible, the temperature of fluidic cell is stabilized.

An example of such an interaction is the self-ionization, where the external electric field changes equilibrium condition of dissociation and recombination of H_3O^+ and H^- [14]. As mentioned above, the mechanism of self-ionization is of quantum nature [6] (among other factors). It should be noted that the expression (5) can include different components, such as a non-stationarity of fluidic cell and external excitations, as well as a non-stationarity of the measurement itself. These components should be distinguished from each other.

Let us consider one of components k, represented, for example, by the magnitude of impedance $Z(f,t)$ with the dimension $Ohm \cdot m$. The measurement of this value by the RMS approach consists in analyzing the excitation signal $V_V(f,t)$ and the current response signal $V_I(f,t)$

$$Z(f,t) = s(f)\frac{V_V(f,t)}{V_I(f,t)}, \tag{6}$$

where $s(f)$ is the cell constant, defined as the ratio between the area of electrodes to the distance between them (considering the geometry of the cell). Since the impedance of a two-terminal network should be independent of time, the following agreement is used – the measurement (6) should be performed in a short time, so that the non-linear part of (5) remains small and can be neglected for the given measurement accuracy

$$Z(f,t) = s(f)\frac{V_V(f,t)}{V_I(f,t)} \underset{t\to 0}{\Longrightarrow} Z(f) = s(f)\frac{V_V(f)}{V_I(f)}. \tag{7}$$

To avoid the nonlinearity in $s(f)$, the frequency f is often fixed. For example, the cell constant is calibrated in this way. It is obvious that (7) and (1) to some extent represent different EIS paradigms, because (1) affects the stationarity of physical quantities indexed by k.

III. Normalization of the response of the test system

Spectroscopy in the form (1) is not used in cases where the structures (2) and (3) are not distinguished from each other. Here, the method (7) is more preferable. However, in applications where structures (2) and (3) should be distinguished, it is necessary to solve the above-mentioned problems of ${}^k\Upsilon_t^f$ in the form of different scales in the index f and to preserve stationarity in the index t. The work [10] already expressed the idea that the structure (2) in ${}^k\Upsilon_t^f$ represents an independent physical quantity characterizing the reaction of test system without external stimuli. In order to avoid different scales in f, it was suggested to make ${}^k\Upsilon_t^f$ (2) in the area A dimensionless with respect to physical quantities in k, for example, in the form

$$\varphi^A = \frac{{}^k\Upsilon_t^{f=f_0\dots f_{max}}}{{}^k\Upsilon_{t_0}^{f=f_0\dots f_{max}}} = func(f,t), \quad t < t_m, \tag{8}$$

so that

$$\varphi^A(f,t) \approx 1, \quad t < t_m. \tag{9}$$

This representation is shown in Fig. 3. The value of t_m is chosen to satisfy (9), which is implemented as a sliding window. Fig. 6 shows the application of (9) to the region B (the dynamics after impact), where the sliding window method allows showing time-frequency patterns

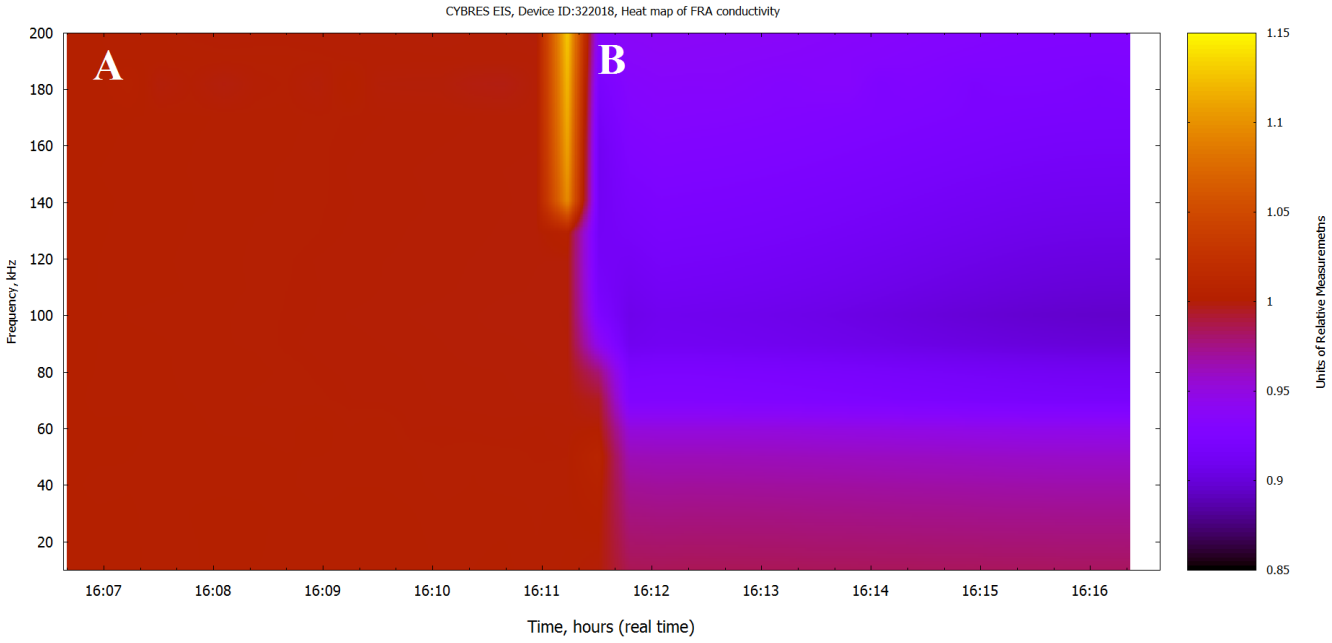

Fig. 4. The normalized representation of the tensor ${}^{k}\varphi_t^f$ by (14) with structures (2) (the region A before exposure) and (3) (the region B after begin of exposure). The electrochemical test system is affected by external thermal excitation.

at the deviation level 10^{-3} Units of Relative Measurements (URM) for all f. In this case, the approximation accuracy (to the 1) of the unexcited state of the EIS system can be defined, for example, the deviation values $10^{-4} - 10^{-5}$ URM are achievable. Considering (9) from the metrological point of view, we can note that (8) acts as a normalizing metric operator with (9) as a unit scale. Although $\varphi(f,t)$ is a function of frequency and time, the normalization (9) makes it, and correspondingly the entire scale, dimensionless that satisfies the assumptions made in [10].

Now we consider the structure (3) in ${}^{k}\Upsilon_t^f$. Its physical meaning is the reaction of test system in the context of physical quantities indexed by k. Here the normalization (9) can not be performed. There are two ways of considering the structure (3) with respect to the structure (2) (the unit scale). In the first case, we extend (8) to all values of t

$$\varphi^B = \left.\frac{{}^{k}\Upsilon_t^{f=f_0\cdots f_{max}}}{{}^{k}\Upsilon_{t_0}^{f=f_0\cdots f_{max}}}\right|_{t=t_w} = func(f), \quad t \le t_{max}, \tag{10}$$

by fixing the time $t = t_w$ in the manner (7). In this method, the entire response of the test system represents the sum of responses at short discrete instants of time, i.e. the value t is replaced by a measurement index. An example can be given by the Nyquist diagram, which does not include time but can be indexed by the number of iterative measurements. This approach solves the problem of measurement stationarity since all indexed values are independent measurements performed in the manner of (7).

In the second case, we consider (8) only for $t \ge t_m$

$$\varphi^B = \frac{{}^{k}\Upsilon_t^{f=f_0\cdots f_{max}}}{{}^{k}\Upsilon_{t_0}^{f=f_0\cdots f_{max}}} = func(f,t), \quad t \ge t_m. \tag{11}$$

Here the whole system is considered as non-stationary in sense of (5) and the dynamics of physical quantities in the index k is investigated. For example, the conductivity dynamics measured by the RMS method can be considered.

Despite the similarity, the (10) and (11) have different metrological and physical meaning, since they lead to different dimensions of the total φ for $t \le t_{max}$

$$\varphi = \varphi^B, \quad t \le t_{max}, \tag{12}$$

and

$$\varphi = \frac{\varphi^A}{\varphi^B} = \frac{1}{\varphi^B}, \quad t \le t_{max}, \tag{13}$$

Both variants convert (10) to the form

$$\left|\begin{array}{cccc|cccc} 1 & 1 & \dots & 1 & {}^{k}\varphi_{t_m}^{f_{max}} & {}^{k}\varphi_{t_{m+1}}^{f_{max}} & \dots & {}^{k}\varphi_{t_{max-1}}^{f_{max}} & {}^{k}\varphi_{t_{max}}^{f_{max}} \\ 1 & 1 & \dots & 1 & {}^{k}\varphi_{t_m}^{f_{max-1}} & {}^{k}\varphi_{t_{m+1}}^{f_{max-1}} & \dots & {}^{k}\varphi_{t_{max-1}}^{f_{max-1}} & {}^{k}\varphi_{t_{max}}^{f_{max-1}} \\ \dots & \dots & \dots & \dots & \dots & \dots & \dots & \dots & \\ 1 & 1 & \dots & 1 & {}^{k}\varphi_{t_m}^{f_2} & {}^{k}\varphi_{t_{m+1}}^{f_2} & \dots & {}^{k}\varphi_{t_{max-1}}^{f_2} & {}^{k}\varphi_{t_{max}}^{f_2} \\ 1 & 1 & \dots & 1 & {}^{k}\varphi_{t_m}^{f_1} & {}^{k}\varphi_{t_{m+1}}^{f_1} & \dots & {}^{k}\varphi_{t_{max-1}}^{f_1} & {}^{k}\varphi_{t_{max}}^{f_1} \\ 1 & 1 & \dots & 1 & {}^{k}\varphi_{t_m}^{f_0} & {}^{k}\varphi_{t_{m+1}}^{f_0} & \dots & {}^{k}\varphi_{t_{max-1}}^{f_0} & {}^{k}\varphi_{t_{max}}^{f_0} \end{array}\right| \tag{14}$$

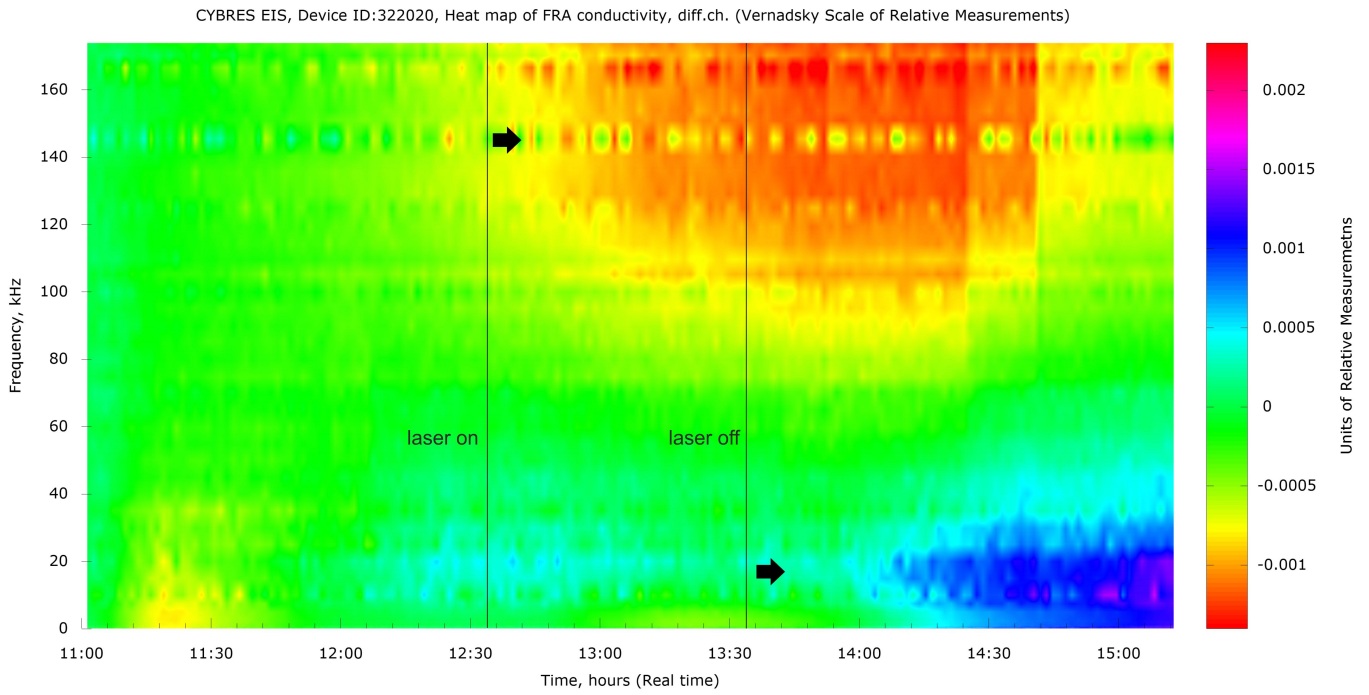

Fig. 5. The impact of a laser (512nm, 5mV, the class 1) on a liquid in the channel 1, the channel 2 is placed behind the channel 1 at the distance of 10 cm. The differential dynamics of channels before, during and after the exposure is shown, the color palette HSV, the resolution $3 \cdot 10^{-3}$ URM for the whole scale. The appearance of high-frequency components after switching on the laser and low-frequency components after switching off is visible. The renormalization ${}^{k}\varphi_t^f$ is performed at the beginning of measurement.

Although φ in (12) is a function of frequency, both time and frequency are represented by discrete measurement indexes. In the physical sense, the expression (10) leads φ to an indexed dimensionless value. On the other hand, φ in (13) has a dimension $func(f,t)^{-1}$ that with similar consideration of frequency as the indexed parameter can lead to $func(t)^{-1}$. Both options are already mentioned in the literature, e.g. [10], [15] expressed arguments in favor of the dimensionless φ, while [16], [17] considered the option sec^{-1} for φ.

IV. Dimension φ: dimensionless quantity, $func(t)^{-1}$ or $func(f,t)^{-1}$?

The physical meaning of φ for $t \leq t_{max}$ consists either in characterization of the test object (when the affecting parameter is known), or in characterization of the affecting parameter (when test object is known). Both variants are used in practical tasks. In our case, with a known test object (e.g. distilled water), it is possible to characterize affecting chemical, biological and biophysical effects (e.g. biological effects of electromagnetic emissions). It seems more logical to use the dimensionless variant of calculating φ, as *the ratio of the behavior of non-affected test system to the behavior of affected test system*. It is necessary to fix the time of impact $t = t_w$. The entire scale based on normalization (8) and (9), and proposed in [10] is dimensionless. The situation with dimensionless scales has not changed in the last 20 years of biophysical research [15].

Dimensionless scales have strengths and weaknesses. For example, without theoretical foundation of biophysical effects that is accepted by most researchers, and with increasing role of quantum effects in macro-systems, a dimensionless scale remains only one realistic possibility for calibrating biophysical measurement devices. Dimensionless scales allow measuring the steady-state characteristics in the response of test systems. However, when considering the dynamics of these responses for $t \geq t_m$, for example, the attenuation values, it is necessary to take $func(f,t)^{-1}$ for φ.

The obvious difficulty of introducing $func(f,t)^{-1}$ is an unclear physical meaning of this dimension. The work [16] provided arguments for $func(t)^{-1}$ with the rotation of objects, which are too complex for solving metrological problems in real devices. An essential argument for the choice of scales is a stationarity of measurement processes (to distinguish with the stationarity of the test system and the impact). The method (7) guarantees such a stationarity, which leads to the selection of (10) and (12) in calculation of φ for $t \leq t_{max}$. This results in a dimensionless scale represented on the corresponding axis as 'Units of Relative Measurements' (URM).

We can give an example. Let the changes in conductivity (phase, correlation, pH, etc.) in the phase B (after the impact) be at 0.999-1.001 URM. These values are obtained according to (10) and (12) as the ratio of conductivity in the experimental region to the conductivity in the background region. In absolute scale, if the conductivity of

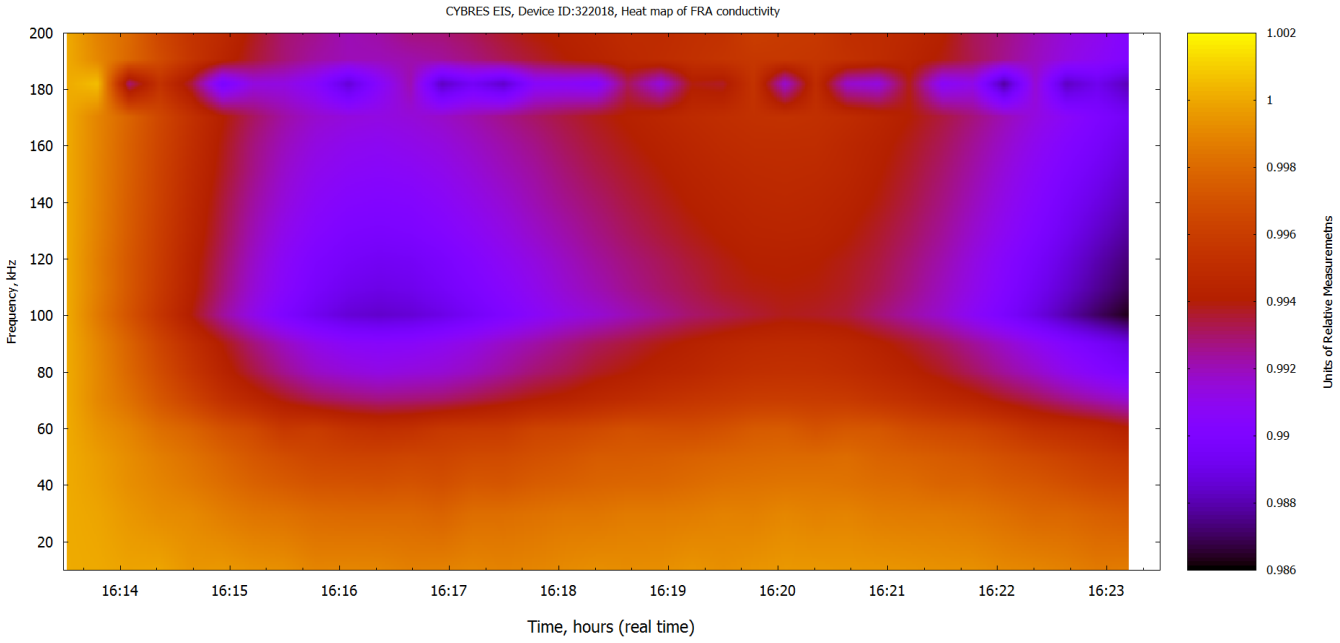

Fig. 6. Appearance of post-experimental time-frequency structures in a test fluid upon renormalization of ${}^{k}\varphi_t^f$ in a sliding analysis window, the color palette RGB.

used water is 2 μS/cm, this means that the variation in experimental region will be 2*(1.001-0.999)=0.004 μS/cm or 4nS/cm. Values in the URM scale allow avoiding different physical quantities and focusing on their relative changes under external excitation. It should be remembered that these quantities are meaningful only with accumulation of statistics from different excitations and test systems.

In conclusion of this section, we would like to quote the words of V.I.Vernadsky: 'On the basis of new physics, the phenomenon should be studied in a space-time domain. The space of life, as we have seen, has its own special state in nature. The time that corresponds to it has not only the polar character, but also a special parameter peculiar to it, a unit of measurement, which is related to life' [11].

V. Calibration of EIS

The expression (9) defines the meaning of calibration, its value for $t \leq t_m$ should approach 1 with the deviation $10^{-3} - 10^{-5}$. It is proposed to use technical demineralized water (for example, meeting the standards of DIN 43530-4, VDE 0510 or similar) at room temperature 22-32°C as a test object. The temperature of liquids (small changes in conductivity can be compensated by means of temperature coefficients) should be also measured. The conductivity of water is recommended to be $1 - 3\mu S/cm$ (therefore it is necessary to control storage conditions with respect to CO_2 and light). It is necessary to exclude light and EM fields from active phase of measurements. An essential issue for calibration is the stationarity condition of the measuring liquid. Omitting the discussion about whether the EIS is stationary in a long time, we point to (7) as a condition for achieving stationarity at such time intervals when (9) is satisfied. In other words, measurements should be conducted with fresh water taken from a large container, the longer the measurement lasts, the greater is the non-stationarity the test fluid. It should be remembered that the exposure of liquids by experimental factors is also not stationary in many cases, therefore, EIS measurements have a probabilistic character. It is necessary to carry out a minimum number of independent measurements (30 attempts) under similar conditions to obtain a statistically significant result.

From a practical point of view, the renormalization of ${}^{k}\varphi_t^f$ can be carried out in a sliding window, and the resolution of post-experimental dynamics is significantly increased, as for example shown in Fig. 6. On the other hand, without renormalization, it is possible to compare the parameters of two different effects, as shown in Fig. 7(a), 5 or as 4D graph in Fig. 7(b).

VI. Conclusion

This paper considered two issues of extended EIS measurements: satisfying the stationarity condition for impedance calculation of EIS in time-frequency domain, and characterization of external excitations without expressing them in electrochemical units. Both problems have common roots in the metrology of EIS. It is demonstrated, that the normalization operator imposes a specific metric on the result and can be expressed either in dimensionless units, or as inverse functions of time (or frequency-time). In this paper, the use of dimensionless units is argued: firstly, they satisfy the stationarity condition, and secondly, they are more consistent with the philosophical idea of the universal characteristic of various biophysical processes. However, it needs to mention that universal measurement scales expressed as $func(t)^{-1}$, $func(f,t)^{-1}$

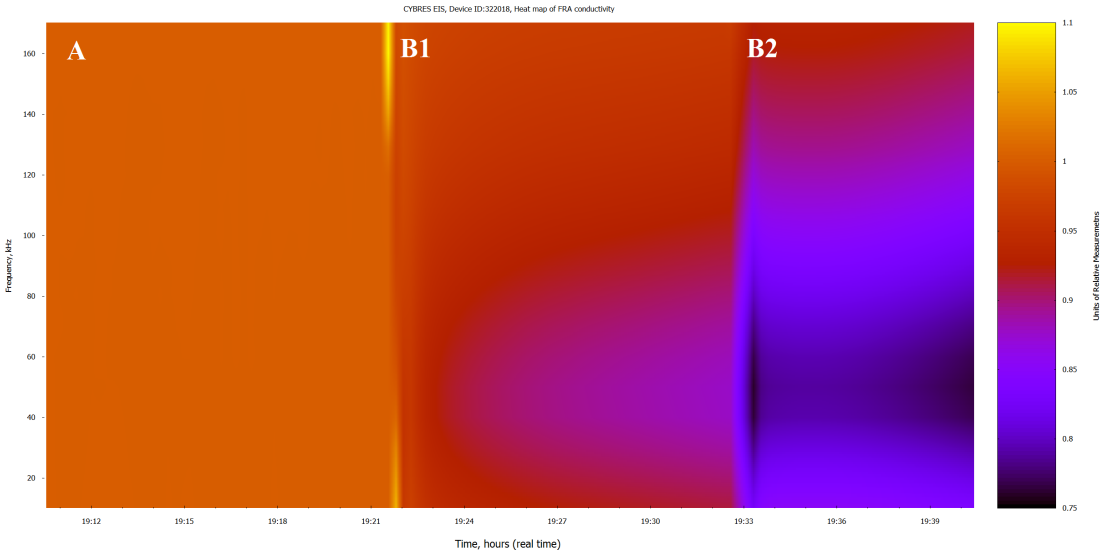

(a)

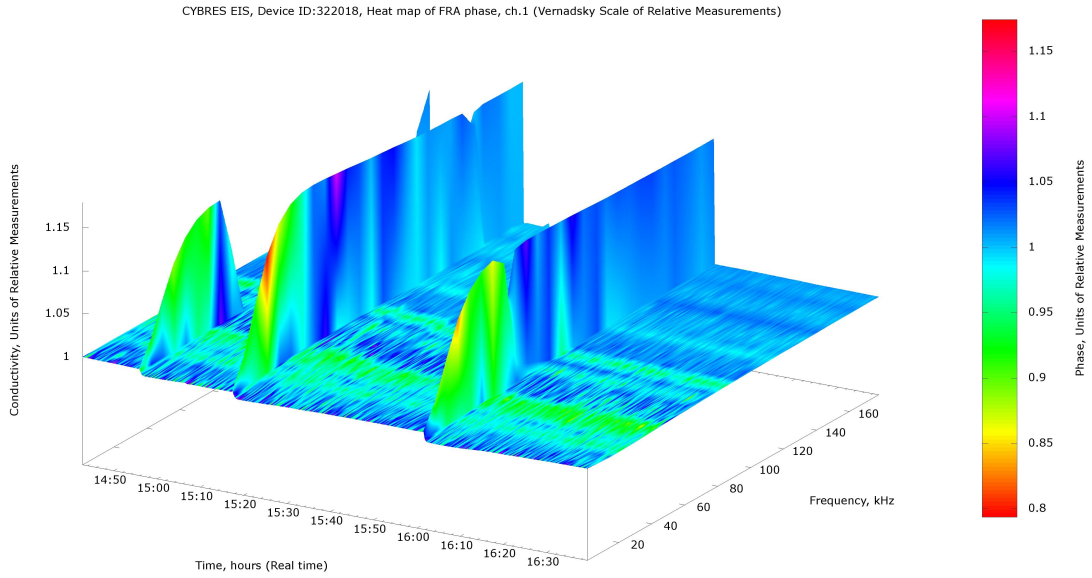

(b)

Fig. 7. **(a)** Two impacts (B1, B2) by biological objects on the test fluid without repeated renormalization ${}^{k}\varphi_t^f$, the differences in the time-frequency properties of both impacts are clearly visible; **(b)** The representation of RMS conductivity and FRA phase of impedance in dimensionless scale in the form of 4D graph, renormalization of ${}^{k}\varphi_t^f$ was carried out once at the beginning of measurement (HSV the color palette). The change in fluid parameters under periodic impact and their returning to the previous level are shown.

has been already discussed in the research community despite their physical meaning needs further clarification.

References

[1] S. Kernbach, I. Kuksin, and O. Kernbach. Analysis of ultraweak interactions by electrochemical impedance spectroscopy (rus). *IJUS*, 11(4):6–22, 2016.

[2] S. Kornienko, O. Kornienko, and P. Levi. Multi-agent repairer of damaged process plans in manufacturing environment. In *Proc. of the 8th Conf. on Intelligent Autonomous Systems (IAS-8), Amsterdam, NL*, pages 485–494, 2004.

[3] P. Boškoski, A. Debenjak, and B.M. Boshkoska. *Fast Electrochemical Impedance Spectroscopy: As a Statistical Condition Monitoring Tool*. Springer Briefs in Applied Sciences and Technology. Springer International Publishing, 2017.

[4] V.A. Sokolova. *First experimental confirmation of torsion fields and their usage in agriculture (rus)*. Moscow, 2002.

[5] Jeremy O. Richardson, Cristóbal Pérez, Simon Lobsiger, Adam A. Reid, Berhane Temelso, George C. Shields, Zbigniew Kisiel, David J. Wales, Brooks H. Pate, and Stuart C. Althorpe. Concerted Hydrogen-Bond Breaking by Quantum Tunneling in the Water Hexamer Prism. *Science*, 351(6279):1310–1313, March 2016.

[6] P. L. Geissler, C. Dellago, D. Chandler, J. Hutter, and M. Parrinello. Autoionization in Liquid Water. *Science*,

291:2121–2124, March 2001.

[7] J.O.M. Bockris and A.K.N. Reddy. *Modern Electrochemistry: An Introduction to an Interdisciplinary Area*. Number Bd. 2 in A Plenum/Rosetta edition. Springer US, 1973.

[8] J.P. Hespanha. *Linear System Theory*. Princeton university press, 2009.

[9] S. Kernbach and O. Kernbach. Reliable detection of weak emissions by the EIS approach. *IJUS*, 14(4):65–79, 2017.

[10] S. Kernbach. On metrology of systems operating with 'high-penetrating' emission (rus). *IJUS*, 1(2):76–91, 2013.

[11] V.I. Vernadsky. *Studying the phenomena of life and the new physics (1931) (Rus)// Proceedings on biogeochemistry and geochemistry of soils*. Moscow, 1992.

[12] P. Levi, M. Schanz, S. Kornienko, and O. Kornienko. Application of order parameter equation for the analysis and the control of nonlinear time discrete dynamical systems. *Int. J. Bifurcation and Chaos*, 9(8):1619–1634, 1999.

[13] S. Kernbach, I. Kuksin, and O. Kernbach. On accurate differential measurements with electrochemical impedance spectroscopy. *WATER*, 8:136–155, 2017.

[14] J.Koryta and J.Dvorak. *Principles of Electrochemistry*. John Wiley & Sons Ltd, 1987.

[15] P.I. Goskov. *Metrological problems of generation and reception of torsion emission*. Reports of the 2nd International Congress, vol.2 / Ed. P.I.Goskov – Barnaul: Publishing house Alt. STU, 1999.

[16] M. Trukhanova and G. Shipov. The Geometro-Hydrodynamical Representation of the Torsion Field. *ArXiv e-prints*, February 2017.

[17] M. Trukhanova. The geometro-hydrodynamical representation of the torsion field. *Physics Letters A (doi: dx.doi.org/10.1016/j.physleta.2017.06.052)*, 2017.